Solid State Communications, Vol. 58, No. 3, pp. 171–176, 1986.
Printed in Great Britain.

0038–1098/86 $3.00 + .00
Pergamon Press Ltd.

ORDERED MAGNETIC FRUSTRATION – V*. ANTIFERROMAGNETIC STRUCTURE OF THE HEXAGONAL BRONZOID HTB–FeF_3; COMPARISON WITH THE NON FRUSTRATED RHOMBOHEDRAL FORM

M. Leblanc, R. De Pape and G. Ferey

Laboratoire des Fluorures, U.A. 449, Faculté des Sciences, 72017 Le Mans Cedex, France

and

J. Pannetier

Institut Laue-Langevin, 156X, 38042 Grenoble Cedex, France

(*Received* 18 *September* 1985 *by E.F. Bertaut*)

A new antiferromagnetic compound HTB–FeF_3 is obtained from the flash evaporation of a solution of iron trifluoride in 49% HF. The nuclear (at 293 and 4.2 K) and the magnetic (at 4.2 K) structures are studied by neutron powder diffraction. The nuclear structure is related to that of the ideal hexagonal tungsten bronze. The symmetry is hexagonal above and below $T_N = 97$ K (293 K: $a = 7.413(2)$ Å, $c = 3.7949(5)$ Å, *SG* $P6/mmm$, $R_N = 0.048$, $R_P = 0.115$, $R_{exp} = 0.057$; 4.2 K: $a = 7.402(1)$ Å, $c = 7.5690(3)$ Å, *SG* $P6_3/m$, $R_N = 0.048$, $R_M = 0.075$, $R_P = 0.113$, $R_{exp} = 0.051$).

The magnetic moments ($\mu = 4.07(8)\mu B$) lie in the basal (0 0 1) plane at 120° one from each other; the interactions between successive Fe^{3+} cations along c are strictly antiferromagnetic. HTB–FeF_3 experiments magnetic frustration in the (0 0 1) planes, related to the existence of triangles of corner sharing Fe^{3+} octahedra in the structure. For sake of comparison, the non frustrated R–FeF_3 is studied, in the temperature range 4.2–406 K, by neutron diffractometry.

INTRODUCTION

CRYSTALS OF $(H_2O)_{0.33}FeF_3$ were recently grown by the hydrothermal method at 360°C, 200 MPa, for 4 days [1]. Their orthorhombic structure results from the stacking of hexagonal tungsten bronze (HTB) type layers (Fig. 1). Only one metallic species, Fe^{3+}, is present and water molecules occupy the center of the hexagonal cavities. Dehydration occurs around 120°C, leading to a new form of iron trifluoride: HTB–FeF_3. This last compound is antiferromagnetic with $T_N \simeq 97$ K, as deduced from Mössbauer measurements. The presence, in the structure, of triangles of metallic atoms, which induces a topological frustration, incited us to examine its influence on the orientation of the spins. Therefore, we determined the nuclear and magnetic structures of HTB–FeF_3 by neutron diffraction. The refinement of the antiferromagnetic structure of the non-frustrated stable rhombohedral form of FeF_3 ($T_N = 365$ K) [2], deriving from the ReO_3 aristotype and hereafter noted R–FeF_3, was also undertaken. Accurate magnetic data of this variety, for which only the orientation of the magnetic moment was previously known, have been established. The magnetic characteristics of the two forms of iron trifluoride are then compared.

EXPERIMENTAL

The large amounts of $(H_2O)_{0.33}FeF_3$, required for neutron techniques, cannot be obtained by the hydrothermal synthesis. Therefore, HTB–FeF_3 samples for neutron diffraction experiments were prepared as follows:

- dissolution of metallic iron in 49% aqueous HF.
- warming of the resulting solution in a platinum cup and oxydation of Fe^{2+} to Fe^{3+} by concentrated HNO_3.
- flash vaporization of the concentrated green syrup at 220°C.
- dehydration of the resulting light-green powder at 150°C under secondary vacuum.

Chemical analysis, within the accuracy of the methods are consistent with the FeF_3 formula (Table 1). Fluorine was analysed with a specific electrode and iron by oxidimetry. Infra-red spectra do not indicate the presence of appreciable amounts of water molecules or hydroxyl groups in the compound.

* For parts I–IV, see refs. 19–22.

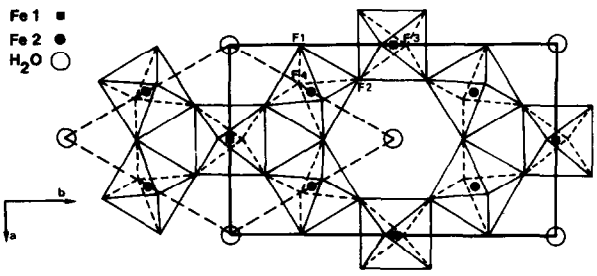

Fig. 1. Projection of one hexagonal tungsten bronze type layer of $(H_2O)_{0.33}FeF_3$.

R–FeF_3 was prepared by the reaction of $FeCl_3$ with gaseous HF at 700°C.

Neutron diffraction patterns were collected on the D1B and D1A powder diffractometers at the Institut Laue-Langevin, using wavelengths of 2.518 and 1.909 Å respectively. The sample was contained in a cylindrical vanadium can (ϕ 15 mm for D1A, ϕ 10 mm for D1B) held in a vanadium tailed liquid helium cryostat or in a furnace with a vanadium heating element for high temperature experiments; the furnace was operating under secondary vacuum ($P \leqslant 10^{-4}$ torr). The high flux and good low angle resolution of D1B allow fast data collection for moderately complex structures; it was used to study the thermal evolution of the R–FeF_3 pattern, in the range 4.2 to 406 K. Diffraction patterns ($14° \leqslant \theta \leqslant 54°$) were collected every 1 K in 6 min. The high resolution of D1A was used to obtain extensive and accurate data for HTB–FeF_3 at three characteristic temperatures (293, 110 and 4.2 K) over a large angular range ($4° \leqslant \theta \leqslant 79°$) in steps of 0.05° 2θ. In the case of HTB–FeF_3, the background is rather high and the counting statistics are relatively poor (Figs. 2, 3). This fact might be due to the presence of a small amount of hydrogen coming from adsorbed water. The peak shape does not deviate from a gaussian profile. Morever, the diffraction patterns reveal the presence of a 20% molar impurity R–FeF_3 [3, 4]. This compound is magnetically ordered just above room temperature and very weak magnetic peaks appear in the 293 K spectrum (noted by an asterisk in Fig. 2). Owing to the high T_N of R–FeF_3, it is assumed that the magnetic moments are almost saturated at 110 K (Fig. 3). Therefore, the contributions of R–FeF_3 cancel in the difference 4.2–110 K pattern (Fig. 3). This difference pattern is characteristic of the magnetic structure of the unique phase HTB–FeF_3. It is noteworthy that HTB–FeF_3

Table 1. Chemical analysis of HTB–FeF_3

	Exp	Calc.
Fe	0.484(15)	0.495
F	0.499(25)	0.505

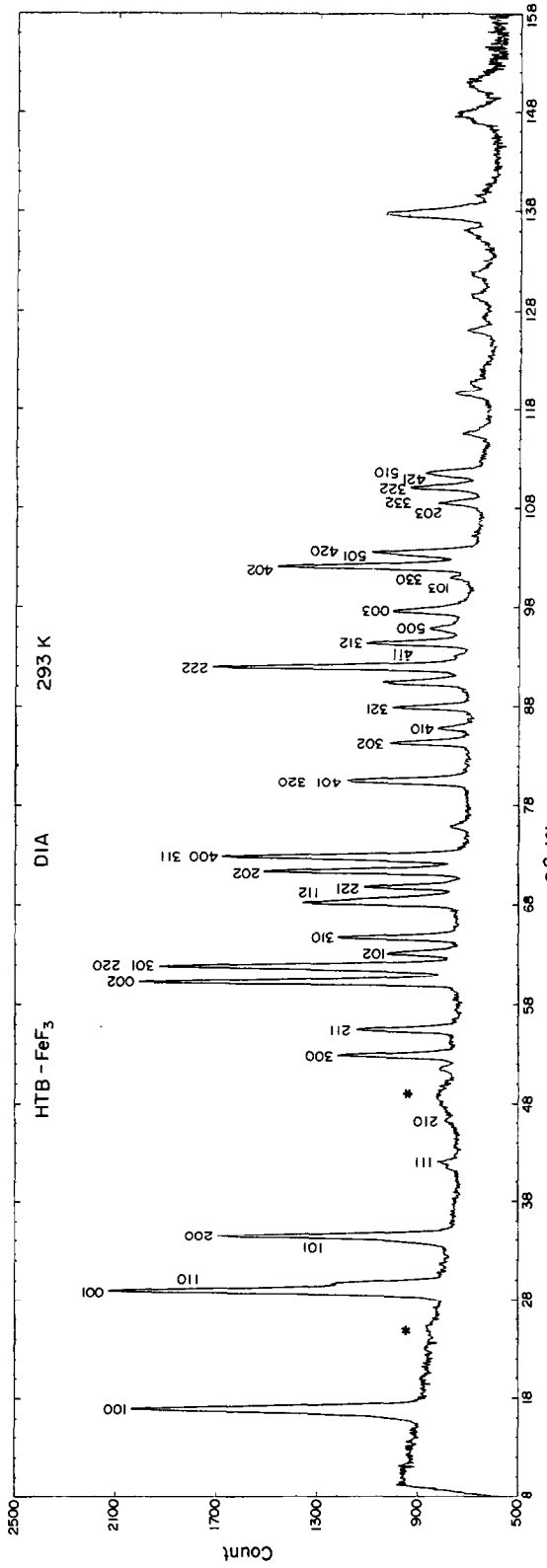

Fig. 2. Neutron diffraction pattern of HTB–FeF_3 at room temperature (λ = 1.909 Å) (* magnetic peaks from R–FeF_3).

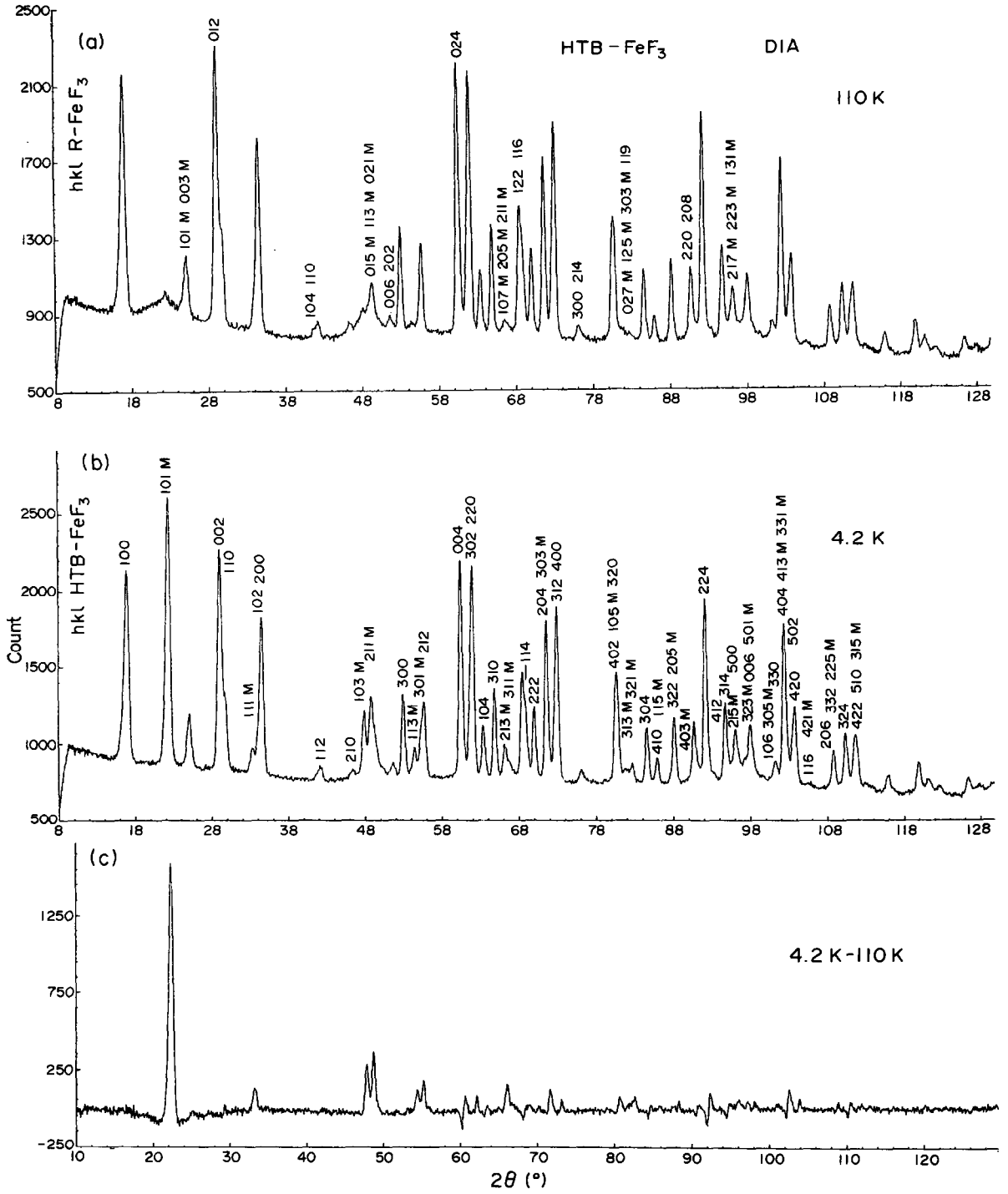

Fig. 3. Neutron diffraction patterns of HTB–FeF_3 at 110 K (a), 4.2 K (b) and difference spectrum 4.2–110 K (c) at $\lambda = 1.909$ Å (D1A). The *hkl* lines of R–FeF_3 and of HTB–FeF_3 (magnetic cell) are indicated in (a) and (b) respectively; the magnetic lines are noted by *M*.

cannot be obtained in large amounts as a pure phase; a different method of preparation, according to Macheteau and Charpin [5], also leads to impurities (20% molar α-Fe_2O_3 and FeF_3, $3H_2O$). For HTB–FeF_3, the spectra were analysed at room temperature and 4.2 K, in the range $2\theta \leqslant 124°$, by the Rietveld method [6] modified by Hewat [7] using the multipatterns profile refinement programs: MPREP, MPROF [8]. For R–FeF_3, the whole angular range of the thermodiffractogram was used for the Rietveld method. The nuclear scattering

Table 2. Refined cell parameters (Å) of HTB–FeF_3

T(K)	a	c	V(Å^3)
293	7.413(2)	3.7949(5)	180.6(2)
4.2	7.402(1)	7.5690(3)	359.1(2)

lengths and magnetic form factors were taken from [9] and [10] respectively.

RESULTS

1. *HTB–FeF_3*

The room temperature pattern of HTB–FeF_3 (Fig. 2) is indexed in an hexagonal cell (Table 2). The absence of systematic extinctions leads to the centric *P6/mmm* space group: HTB–FeF_3 adopts the ideal tungsten bronze type structure [11] with empty tunnels (Table 3). Below the Néel temperature, the symmetry remains hexagonal but the new magnetic lines imply the doubling of the high temperature c parameter (Table 2). At 4.2 K, the magnetic structure was solved using a 6_3 symmetry axis. In this model, a ferromagnetic component is authorized along the 6_3 axis, but ruled out by the magnetization measurements. The spin direction was thereby constrained to lie along the a axis; this minimizes the magnetic dipolar energy. A severe overlap of the HTB–FeF_3 and R–FeF_3 diagrams occurs; however, satisfactory results are obtained with the nuclear space group $P6_3/m$ and with the position of F2

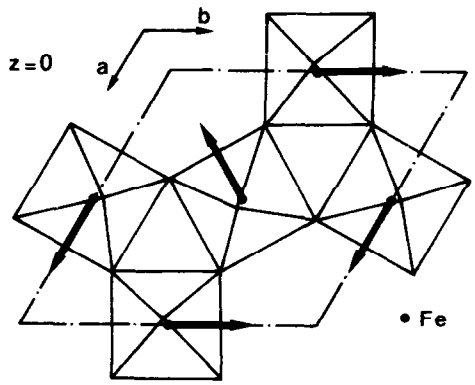

Fig. 4. Magnetic structure of HTB–FeF_3 (layer at $z = 0$).

Table 3. Refined atomic coordinates and thermal parameters in HTB–FeF_3 at room temperature

	x	y	z			
Fe	1/2	0	0			
F1	1/2	0	1/2			
F2	0.2114(5)	−0.2114(5)	0			
	U_{11}	U_{22}	U_{33}	U_{12}	U_{13}	U_{23}
Fe	0.0013(7)	0.001(1)	0.009(1)	0.0005(5)	0	0
F1	0.025 (3)	0.008(4)	0.001(5)	0.004 (2)	0	0
F2	0.0013(8)	0.001(4)	0.024(1)	0.0005(5)	0	0

Table 4. Refined atomic coordinates, thermal parameters, magnetic moment (μB) and selected interatomic distances (Å) and angles (°) in HTB–FeF_3 at 4.2 K

	x	y	z	M		
Fe	1/2	0	0	4.07(8)		
F1	0.496 (3)	0.029 (2)	1/4			
F2	0.2111(2)	−0.2111(2)	0			
	U_{11}	U_{22}	U_{33}	U_{12}	U_{13}	U_{23}
Fe	0.0011(7)	0.0007(7)	0.0088(8)	−0.0004(4)	0	0
F1	0.025 (3)	0.006 (3)	0.001 (4)	0.003 (2)	0	0
F2	0.001 (1)	0.001 (1)	0.024 (1)	−0.0006(5)	0	0

2 x Fe − F1	1.906(8)	F1 − Fe − F1	179.7(3)
4 x Fe − F2	1.917(3)	F1 − Fe − F2	91.1(2)
		F1 − Fe − F2	96.6(2)
⩽ Fe − F ⩾	1.913	F2 − Fe − F2	177.8(1)
		F2 − Fe − F2	89.9(1)

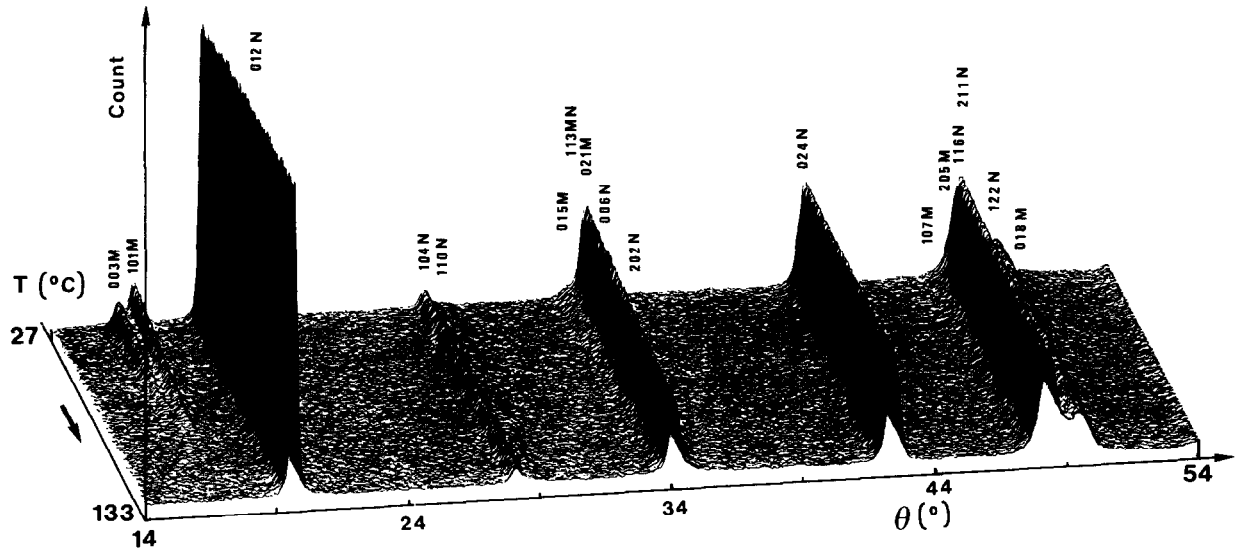

Fig. 5. Neutron thermodiffractogram of R–FeF_3 above room temperature ($\lambda = 2.518$ Å, $\Delta t = 6$ mn, $\Delta T = 1°C$, D1B). *M* and *N* refer respectively to magnetic and nuclear reflections.

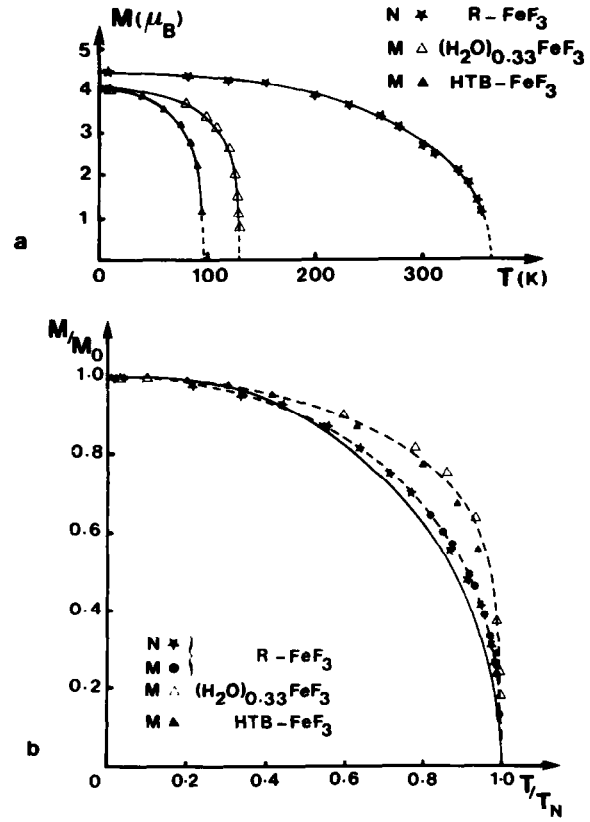

Fig. 6. Comparison of HTB–FeF_3 and R–FeF_3: (a) magnetization at Fe^{3+} site vs temperature, (b) reduced magnetization vs reduced temperature. *M* and *N* correspond to Mössbauer [23] and neutron diffraction experiments respectively. For sake of comparison, $(H_2O)_{0.33}FeF_3$ data [24] are included.

constrained in $(x, -x, 0)$. The final results are given in Table 4. At room temperature and 4.2 K, the reliability factors establish as follows:

T (K)	*R* (Nuclear)	*R* (Magnetic)	*R* (Profile)
293	0.048	–	0.115
4.2	0.048	0.075	0.113
T (K)	R_ω (Profile)	*R* (Expected)	*N* (param)
293	0.101	0.057	28
4.2	0.098	0.051	34

The list of observed and calculated intensities can be obtained upon request to the authors.

At 4.2 K, the nuclear structure does not differ significantly from the room temperature structure. Large thermal motion parameters are observed for F1 in the (0 0 1) plane, and along *c* for F2. An atomic disorder, due to a very small substitution of F^- by OH^- probably explains this fact. However, no evidence of statistical occupancy of hydrogen positions was found from refinement nor, as previously mentioned, from infra-red spectroscopy.

The magnetic structure is described (Fig. 4) with three magnetic sublattices at 120° one from each other in each (0 0 1) plane; the interactions between successive Fe^{3+} spins are antiferromagnetic along *c* ($\mu = 4.07(8)\mu B$ at 4.2 K).

According to Marland and Betts [12] and Darcy [13], this model is consistent with Heisenberg antiferromagnetic interactions between Fe^{3+}.

2. *R–FeF_3*

The refinement of the D1B diffractogram (Fig. 5) shows that the thermal variation of the parameters (Å) of the hexagonal cell, derived from the rhombohedral cell, is approximately linear in the range 80–406 K with:

$$a = 5.189 + 1.4\ 10^{-4} \times T(\mathrm{K}),$$

$$c = 13.298 - 5.2\ 10^{-5} \times T(\mathrm{K}).$$

No noticeable variation of the thermal expansion coefficients occurs at T_N (2). This Néel temperature is shown by the vanishing of the magnetic peaks, noted *M* in Fig. 5, around 365 K.

The antiferromagnetic structure was refined at fourteen temperatures. As previously described [14, 15], the spins of Fe^{3+} lie in the (0 0 1) plane of the hexagonal cell and adopt a *G* type arrangement [16]. The ferromagnetic component along *c* ($1.5\ 10^{-2}\ \mu B$), previously observed from magnetization measurements [17] could not be refined from the D1B data. At 4.2 K, the moments adopt a value $\mu = 4.45(4)\mu B$ in good agreement with the previous data of Jacobson ($\mu = 4.52(5)\mu B$) [15].

The thermal evolution of the magnetic moment (Fig. 6) does not depart from a Brillouin law $B(J = 5/2)$ and no magnetic phase transition is observed between T_N and 4.2 K on the diffractogram. This rules out a previous assumption deduced by Shane [18] from AFMR experiments: the hard magnetization *c* axis was supposed to change in an easy axis below 251 K.

3. COMPARISON OF THE MAGNETIC DATA OF HTB–FeF_3 AND R–FeF_3 IN TERMS OF MAGNETIC FRUSTRATION

The comparison of the two varieties of iron trifluoride shows that in HTB–FeF_3, despite a stable magnetic structure, magnetic frustration (19–22) is effective: the Néel temperature drops from 365 K in R–FeF_3 (2, 23) to 97 K in HTB–FeF_3 [24] [Fig. 6(a)]. In addition, at 4.2 K, the hyperfine magnetic field at the iron nucleus decreases from 618 kOe [2, 23] in R–FeF_3 to 560 kOe in HTB–FeF_3 [24]; correlatively, a reduction of the magnetic moment at 4.2 K is observed ($(4.45(4))\mu B$ and $4.07(8))\mu B$ respectively). It is also noteworthy that the reduced magnetization as a function of the reduced temperature [Fig. 6(b)] deviates strongly from the Brillouin function $B(J = 5/2)$ in HTB–FeF_3 or in $(H_2O)_{0.33}FeF_3$ but only slightly in the case of R–FeF_3.

REFERENCES

1. M. Leblanc, G. Ferey, P. Chevallier, Y. Calage & R. De Pape, *J. Solid State Chem.* **47**, 53 (1983).
2. G.K. Wertheim, H.J. Guggenheim & D.N.E. Buchanan, *Solid State Commun.* **5**, 537 (1967).
3. M.A. Hepworth, K.H. Jack, R.D. Peacock, G.J. Westland, *Acta Crystallogr.* **10**, 63 (1957).
4. M. Leblanc, J. Pannetier, G. Ferey & R. De Pape, *Rev. Chim. Miner.* **22**, 107 (1985).
5. Y. Macheteau & P. Charpin, *C.R. Acad. Sci.* **275C**, 443 (1972).
6. H.M. Rietveld, *J. Appl. Crystallogr.* **2**, 65 (1969).
7. A.W. Hewat, Harwell Report AERE-R 7350 (1973).
8. M.W. Thomas & P.J. Bendall, *Acta Crystallogr.* **A34**, S351 (1978).
9. L. Koester & H. Rauch, IAEA contract 2517/RB (1981).
10. R.E. Watson & J. Freeman, *Acta Crystallogr.* **14**, 27 (1961).
11. A. Magneli, *Acta. Chem. Scand.* **7**, 315 (1953).
12. L.G. Marland & D.D. Betts, *Phys. Rev. Lett.* **43**, 1618 (1979).
13. L. Darcy, P.J. Wojtowicz & M. Rayl, *Mater. Res. Bull.* **8**, 515 (1973).
14. E.O. Wollan, H.R. Child, W.C. Koehler & M.K. Wilkinson, *Phys. Rev.* **112**, 1132 (1958).
15. A.J. Jacobson, L. McBride & B.E.F. Fender, *J. Phys.* **C7**, 783 (1974).
16. E.F. Bertaut, *Magnetism III*, (Edited by Rado & Shull), 149 (1963).
17. J.M. Dance, Thèse 3ème cycle Bordeaux (1973).
18. J.R. Shane & M. Kestigian, *J. Appl. Phys.* **39(2)**, 1027 (1968).
19. G. Ferey, R. De Pape & B. Boucher, *Acta Crystallogr.* **B34**, 1084 (1977).
20. G. Ferey, M. Leblanc, R. De Pape & J. Pannetier, *Solid State Commun.* **53**, 559 (1985).
21. G. Ferey, M. Leblanc, R. De Pape & J. Pannetier, *Spin frustration problems in fluorides*, p. 395, *Inorganic Fluorides: chemistry and physics*, (Edited by P. Hagenmuller), Academic Press (1985).
22. Y. Laligant, M. Leblanc, J. Pannetier & G. Ferey, *J. Phys. C* (submitted).
23. G.K. Wertheim, H.J. Guggenheim & D.N.E. Buchanan, *Phys. Rev.* **169(2)**, 169 (1968).
24. Y. Calage, M. Leblanc, G. Ferey & F. Varret, *J. Magn. Magn. Mat.* **43**, 195 (1984).